Molecular Phylogenetics and Evolution 137 (2019) 300–312

Contents lists available at ScienceDirect

Molecular Phylogenetics and Evolution

journal homepage: www.elsevier.com/locate/ympev

Biogeography of *Mesalina* (Reptilia: Lacertidae), with special emphasis on the *Mesalina adramitana* group from Arabia and the Socotra Archipelago

Marc Simó-Riudalbas[a,*], Karin Tamar[a], Jiří Šmíd[b,c], Pelagia Mitsi[a], Roberto Sindaco[d], Laurent Chirio[e], Salvador Carranza[a]

[a] Institutute of Evolutionary Biology (CSIC-Universitat Pompeu Fabra), Passeig Maritím de la Barceloneta, 37-49, 08003 Barcelona, Spain
[b] Department of Zoology, National Museum, Cirkusová 1740, Prague, Czech Republic
[c] Department of Zoology, Faculty of Science, Charles University in Prague, Viničná 7, Prague, Czech Republic
[d] Museo Civico de Storia Naturale, via San Francesco di Sales 188, I-10022 Carmagnola, Torino, Italy
[e] 14 Rue des Roses, 06130 Grasse, France

ARTICLE INFO

Keywords:
Allopatry
Arabian Peninsula
Endemicity
Land bridge
Lacertids
Niche modelling
Speciation

ABSTRACT

The lacertid lizards of the genus *Mesalina* inhabit the arid regions of the Old World, from North Africa to NW India. Of the 19 recognized species within the genus, eleven occur in Arabia. In this study, we explore the genetic variability and phylogeographic patterns of the less studied *M. adramitana* group from southern Arabia and the Socotra Archipelago within the phylogenetic and biogeographic context of the entire genus. Our unprecedented sampling extends the distribution ranges of most *Mesalina* species and, for the first time, sequences of *M. ayunensis* are included in a phylogenetic analysis. We perform analyses of concatenated multilocus datasets and species trees, conduct species delimitation analyses, and estimate divergence times within a biogeographic framework. Additionally, we inferred the environmental suitability and identified dispersal corridors through which gene flow is enabled within *M. adramitana*. Our results show that the Socotra Archipelago was colonized approximately 7 Mya by a single oversea colonization from mainland Arabia. Then, an intra-archipelago dispersal event that occurred approximately 5 Mya resulted in the speciation between *M. balfouri*, endemic to Socotra, Samha and Darsa Islands, and *M. kuri*, endemic to Abd al Kuri Island. Similar to previous studies, we uncovered high levels of genetic diversity within the *M. adramitana* species-group, with two highly divergent lineages of *M. adramitana* living in allopatry and adapted to locally specific climatic conditions that necessitate further investigation.

1. Introduction

Mesalina Gray, 1838 is a Saharo-Sindian lacertid genus widespread across North Africa, the Middle East, and the Iranian Plateau, eastwards to Pakistan, with some species reaching the Sahel, the Horn of Africa and the Socotra Archipelago (Fig. 1). Currently, the genus comprises 19 species and is the third most diverse genus within the Eremiadini tribe of the family Lacertidae, after *Acanthodactylus* and *Eremias* (Arnold et al., 2007; Uetz et al., 2017). All *Mesalina* species are small, fast, ground-dwelling, diurnal lizards well adapted to desert and xeric shrublands.

Taxonomic studies of *Mesalina* have been hampered by the wide geographic distribution of the genus, including several politically unstable regions, and the existence of several genetically highly divergent species complexes, some of them with paraphyletic and polyphyletic species and relatively high levels of cryptic diversity (Kapli et al., 2008, 2015; Šmíd and Frynta, 2012). Despite these problems, recent systematic revisions shed light on two of these species complexes (*M. brevirostris* and *M. guttulata*; Šmíd et al., 2017; Sindaco et al., 2018, respectively). At present, all *Mesalina* taxa can be divided according to their phylogenetic relationships into the following seven assemblages: (i) *M. watsonana*, (ii) *M. martini*, (iii) the still unrevised *M. olivieri* species complex, (iv) *M. rubropunctata*, (v) the *M. adramitana* group, (vi) the *M. brevirostris* group and (vii) the *M. guttulata* group. The latter three groups occur throughout the Arabian Peninsula, an area that has played a crucial role in shaping the current diversity and geographical distribution of the fauna inhabiting Africa and Eurasia (i.e., Šmíd et al., 2013; Metallinou et al., 2012, 2015; Tamar et al., 2016a, 2016b, 2018).

The Arabian Peninsula has a complex geological history and varying levels of connectivity with Africa and Eurasia that have enabled ancient

* Corresponding author.
E-mail address: marcsimo88@gmail.com (M. Simó-Riudalbas).

https://doi.org/10.1016/j.ympev.2019.04.023
Received 8 June 2018; Received in revised form 24 April 2019; Accepted 24 April 2019
Available online 25 April 2019

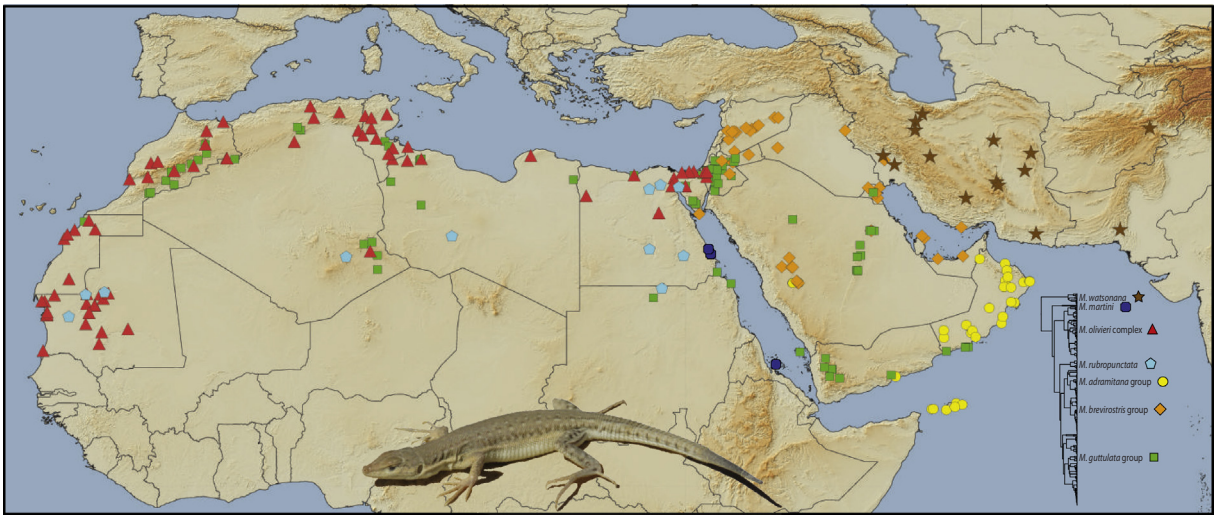

Fig. 1. Localities of the *Mesalina* samples included in this study. Colors correspond to groups visualized in the lower right tree (same tree as Fig. 2A). Inset picture shows a specimen of *M. adramitana* from northern Oman.

vicariance splits and uneven movements of terrestrial fauna across open seas or land bridges (Bohannon, 1986; Bosworth et al., 2005; Fernandes et al., 2006). The tectonic separation between Arabia and Africa resulted in the formation of the Red Sea and the Gulf of Aden during the late Oligocene (23–31 million years ago [Mya]; Bosworth et al., 2005). This continental break-up triggered the separation of the Socotra Archipelago from the Dhofar region in southern Oman approximately 24 Mya (Autin et al., 2010; Fournier et al., 2010). Subsequently, the collision between the Arabian plate with Eurasia led to the gradual closure of the Tethyan Seaway and the formation of the *Gomphotherium* land bridge during the Early-Middle Miocene (around 15–18 Mya; Harzhauser et al., 2007; Harzhauser and Piller, 2007; Rögl, 1999). In turn, sea level fluctuations during the Miocene (~6–14 Mya) permitted the formation of temporary land connections between Africa and Arabia (Haq et al., 1987; Jones, 1999; Bosworth et al., 2005; Fernandes et al., 2006). Additionally, global climate changes and oscillations during the Cenozoic have also been suggested as one of the main drivers of diversification and distributional patterns of North African and Arabian faunas (e.g., Douady et al., 2003; Guillaumet et al., 2008; Gonçalves et al., 2012; Metallinou et al., 2012, 2015; Šmíd et al., 2013; Tamar et al., 2014, 2016a, 2016b, 2018). It is generally accepted that subsequent aridification processes and climatic fluctuations that occurred during the Miocene and the Pleistocene dramatically altered the landscapes of North Africa and Arabia, triggering the expansion and contraction of desert areas and sand seas (Zachos et al., 2001; Griffin, 2002; Edgell, 2006).

Eleven species of *Mesalina* are currently recognized in Arabia, inhabiting arid and semi-arid areas from sea level up to 3,500 m a.s.l. (see Uetz et al., 2017; Sindaco et al., 2018). Although areas of sympatry occur between some species, their distribution within the Arabian Peninsula is essentially allopatric or parapatric (Arnold, 1980). Apart from the *M. brevirostris* and *M. guttulata* groups, there are four endemic Arabian taxa: *M. adramitana* (Boulenger, 1917), *M. ayunensis* Arnold, 1980, *M. balfouri* (Blanford, 1881), and *M. kuri* Joger and Mayer, 2002, all included within a clade called hereinafter the *M. adramitana* group. The monophyly of this group has been supported in previous studies never including *M. ayunensis* (Joger and Mayer, 2002; Kapli et al., 2015; Tonini et al., 2016). However, the relationships within the *M. adramitana* group are still poorly understood and the biogeographic history of *Mesalina* in the Socotra Archipelago hovers in mystery.

Mesalina adramitana was originally described from the Hadhramaut area in southern Arabia. It is an abundant species, found widely across the southern and western Arabian Peninsula (Sindaco and Jeremčenko, 2008). It has been found inhabiting sandy or gravelly plains with some vegetation, from sea level up to 1300 m (pers. obs.). Despite their capacity to tolerate high temperatures (around 50 °C), adults and juveniles often climb on small shrubs to minimize contact with the hot ground (Arnold, 1980). Although *M. adramitana* includes distinct populations with remarkable morphological differentiation and color variations (especially specimens from Dhofar; Arnold, 1980, 1986a; van der Kooij, 2001), no molecular studies have been carried out to investigate its systematics. On the contrary, the South Arabian *M. ayunensis* is only known from a few localities in Dhofar, where it can occur in sympatry with *M. adramitana* (Arnold, 1980). Little is known on its biology and it has never been included in a molecular phylogenetic analysis. The other two Arabian species of the *M. adramitana* group are exclusively found in the Socotra Archipelago. *Mesalina balfouri* inhabits open flat sandy areas but also gravel and rocky substrates on Socotra, Samha and Darsa Islands and *M. kuri* is only found in flat areas on sandy or hardened ground in Abd al Kuri Island (Razzetti et al., 2011).

The present work aimed to explore the genetic variability and phylogeographic patterns of the largely unstudied *M. adramitana* group within the phylogenetic and biogeographic context of the entire genus. We performed phylogenetic analyses of concatenated multilocus datasets and species trees, conducted species delimitation analyses, and estimated divergence times within a biogeographic framework. Additionally, we infer environmental suitability and identify dispersal corridors through which gene flow is enabled within *M. adramitana*.

2. Materials and methods

2.1. Taxon sampling, datasets, DNA amplification, sequencing and alignment

In total, sequences of 349 *Mesalina* specimens sampled from its entire distribution range were used in this study, including representatives of 18 of the 19 recognized species (Table S1; *M. ercolinii* was not sampled; sequences retrieved from GenBank are from Kapli et al., 2008, 2015; Šmíd et al., 2017; Sindaco et al., 2018). The monophyly and phylogenetic position of *Mesalina* within the tribe Eremiadini was established in previous studies (Mayer and Pavlicev, 2007; Pyron et al., 2013). Therefore, in some analyses we included as outgroups 15 specimens of the genera *Gallotia* (Subfamily Gallotiinae) and *Podarcis* (Subfamily Lacertinae, Lacertini tribe) that were also used for the divergence time estimation (see Tamar et al., 2016a). Sample codes, localities and GenBank accession numbers are given in Table S1.

All sampled localities are shown in Fig. 1. A summary of the four datasets used to address the different objectives of this study is shown in Table S2.

DNA of alcohol-preserved muscle or liver tissue samples was extracted using the SpeedTools Tissue DNA Extraction kit (Biotools, Madrid, Spain). In total, sixty-nine individuals were newly sequenced for up to seven loci (both strands), which included three mitochondrial gene fragments, the ribosomal 12S and 16S rRNA (*12S* and *16S*, respectively), and the protein-coding cytochrome *b* (*cytb*), and four protein-coding nuclear gene fragments: the acetylcholinergic receptor M4 (*ACM4*), the oocyte maturation factor MOS (*c-mos*), the melano-cortin 1 receptor (*MC1R*), and the recombination activating gene 1 (*RAG1*). A complete list of all primers used, PCR conditions and source references is given in Table S3.

Chromatographs were checked, assembled and edited using Geneious v.7.1.9 (Kearse et al., 2012). Heterozygous positions in the nuclear genes were identified and coded according to the IUPAC ambiguity codes. Sequences were aligned for each gene independently using the online application of MAFFT v.7.3 (Katoh and Standley, 2013) with default parameters, except for the *12S* and *16S* fragments to which we applied the Q-INS-i strategy that considers the secondary structure of the RNA. Poorly aligned gap regions of the *12S* and *16S* genes were eliminated with Gblocks (Castresana, 2000) using the less stringent options (Talavera and Castresana, 2007). No stop codons were detected after translation of the protein-coding genes to amino acids, suggesting that all genes are functional and no pseudogenes were amplified. Uncorrected *p*-distances (with pairwise deletion) for the members of the *M. adramitana* group were calculated for the three mitochondrial fragments (*12S*, *16S*, *cytb*) in MEGA v.7 (Kumar et al., 2016).

2.2. Phylogenetic analyses of the genus Mesalina

Dataset 1 was assembled with the objective of inferring the phylogenetic relationships of the genus *Mesalina*. It is the most complete dataset and included 349 specimens of 18 species of *Mesalina* sequenced for up to seven loci (mitochondrial data is available for all specimens; Tables S1 and S2). PartitionFinder v.2 (Lanfear et al., 2016) was used to infer the best partitioning scheme and models of sequence evolution with the following parameters: linked branch length; BEAST models; BIC model selection; all scheme search algorithm; each marker as a data bloc. Phylogenetic relationships within *Mesalina* were inferred under maximum likelihood (ML) and Bayesian inference (BI) frameworks. Prior settings, partitions, and models for the analyses are listed in Table S2. We treated alignment gaps as missing data and the four nuclear genes were not phased. The BI analyses of dataset 1 were performed in BEAST v.1.8.2 (Drummond et al., 2012). The .xml file was manually modified to set useAmbiguities = "true" for the nuclear gene partitions in order to account for variability in the heterozygous positions instead of treating them as missing data. The ML analyses of dataset 1 were carried out in RAxML v.8.1.2 (Stamatakis, 2014) as implemented in raxmlGUI v.1.5 (Silvestro and Michalak, 2012). Reliability of the ML tree was assessed by bootstrap analysis including 1000 replications. In all analyses, nodes were considered well supported if they received ML bootstrap values $\geq$70% and posterior probability (pp) support values $\geq$0.95.

For all the BI analyses of this study (BEAST and *BEAST), convergence was assessed by confirming that all parameters had reached stationarity and had sufficient effective sample sizes (ESS > 200) using Tracer v.1.6 (Rambaut et al., 2014). Results from independent runs were combined in LogCombiner discarding 10% of trees as burn-in and an ultrametric maximum clade credibility tree was produced with TreeAnnotator (both provided with the BEAST package).

2.3. Species delimitation analyses and species-tree

To evaluate the species boundaries within *Mesalina* and within the *M. adramitana* group, we applied a combination of two species delimitation approaches. Mitochondrial divergent lineages were first estimated using the Generalized Mixed Yule-coalescent analysis (GMYC; Pons et al., 2006) and its Bayesian implementation (bGMYC; Reid and Carstens, 2012). These analyses rely on single locus data; therefore, we assembled dataset 2, which included a total of 307 unique haplotypes of the concatenated *16S* and *cytb* sequences, as these two genes include the most complete sampling of individuals (Tables S1 and S2). The mitochondrial phylogenetic tree for dataset 2 was inferred in BEAST as detailed in Table S2, with partitions and models of sequence evolution inferred in PartitionFinder with the same parameters as listed above. The GMYC function was performed using the "splits" package (Ezard et al., 2009) in R3.3.3 (R Core Team, 2017), applying a single threshold. The bGMYC analysis was performed using the R package "bGMYC" (Reid and Carstens, 2012). In this analysis, a random subsample of 250 trees from the posterior distribution of the BEAST runs was used to calculate marginal posterior probabilities of the model. MCMC chains were run for 10^3 generations with a burn-in of the first 10% of trees.

The results of the bGMYC species delimitation analysis of *Mesalina* with dataset 2 were used to define the lineages that should be implemented in the multilocus species-tree of the *M. adramitana* group (see bGMYC results in Fig. S3). The species-tree was inferred in *BEAST (v.1.8.2; Heled and Drummond, 2010) with dataset 3, which included the four independent phased nuclear loci only. Details on the composition of dataset 3 and on the *BEAST analysis are presented in Tables S1 and S2. jModelTest v.2.1.7 (Darriba et al., 2012; Guindon and Gascuel, 2003) was used to select the best model of nucleotide substitution for each locus of dataset 3 under the Bayesian information criterion (BIC). Unfortunately, one of the recovered bGMYC lineages within the *M. adramitana* group had no nuclear sequences (specimens NHMC80.3.142.2, NHMC80.3.142.3, and NHMC80.3.164.8; see Table S1) and therefore this bGMYC lineage was not included in dataset 3.

As a second step of the species delimitation process in the *M. adramitana* group, we carried out a nuclear multilocus Bayesian coalescent species delimitation and species tree analyses performed with Bayesian Phylogenetics and Phylogeography (BP&P v.3.3; Yang and Rannala, 2010) using dataset 3 (see details in Tables S1 and S2). We carried out two analytical approaches: (a) conducting Bayesian species delimitation analyses using a fixed guide tree (the species-tree recovered from *BEAST; see above), (b) implementing a joint analysis conducting Bayesian species delimitation while estimating the species tree (Yang and Rannala, 2014). For both approaches algorithms 0 and 1 were used, assigning each species delimitation model equal prior probability. As the prior distributions of the ancestral population size (θ) and root age (τ) can affect the posterior probabilities of the models (Yang and Rannala, 2010), we tested four different combinations of gamma-distributed priors (see details in Table S2). The locus rate parameter that allows variable mutation rates among loci was estimated with a Dirichlet prior ($\alpha = 2$). Since our dataset was autosomal only, the heredity parameter that allows θ to vary among loci was not used. We ran each rjMCMC analysis twice to confirm consistency between runs. We considered speciation probability values $\geq$0.95 as strong evidence for speciation.

2.4. Divergence times and ancestral range reconstructions

To infer divergence times and to reconstruct the ancestral areas within *Mesalina* we assembled dataset 4. This dataset included one representative of each of the 52 bGMYC lineages of *Mesalina*. For species with bGMYC lineages distributed in more than one discrete biogeographical region, we included specimens representing all occupied regions (i.e., we added a total of 11 specimens for *M. olivieri*, *M. rubropunctata*, *M. brevirostris*, *M. bernoullii*). We also added 15 *Gallotia* and *Podarcis* specimens as outgroups for calibration purposes (Tables S1 and S2). The divergence time estimation and the biogeographic analysis were carried out simultaneously using the Bayesian stochastic search

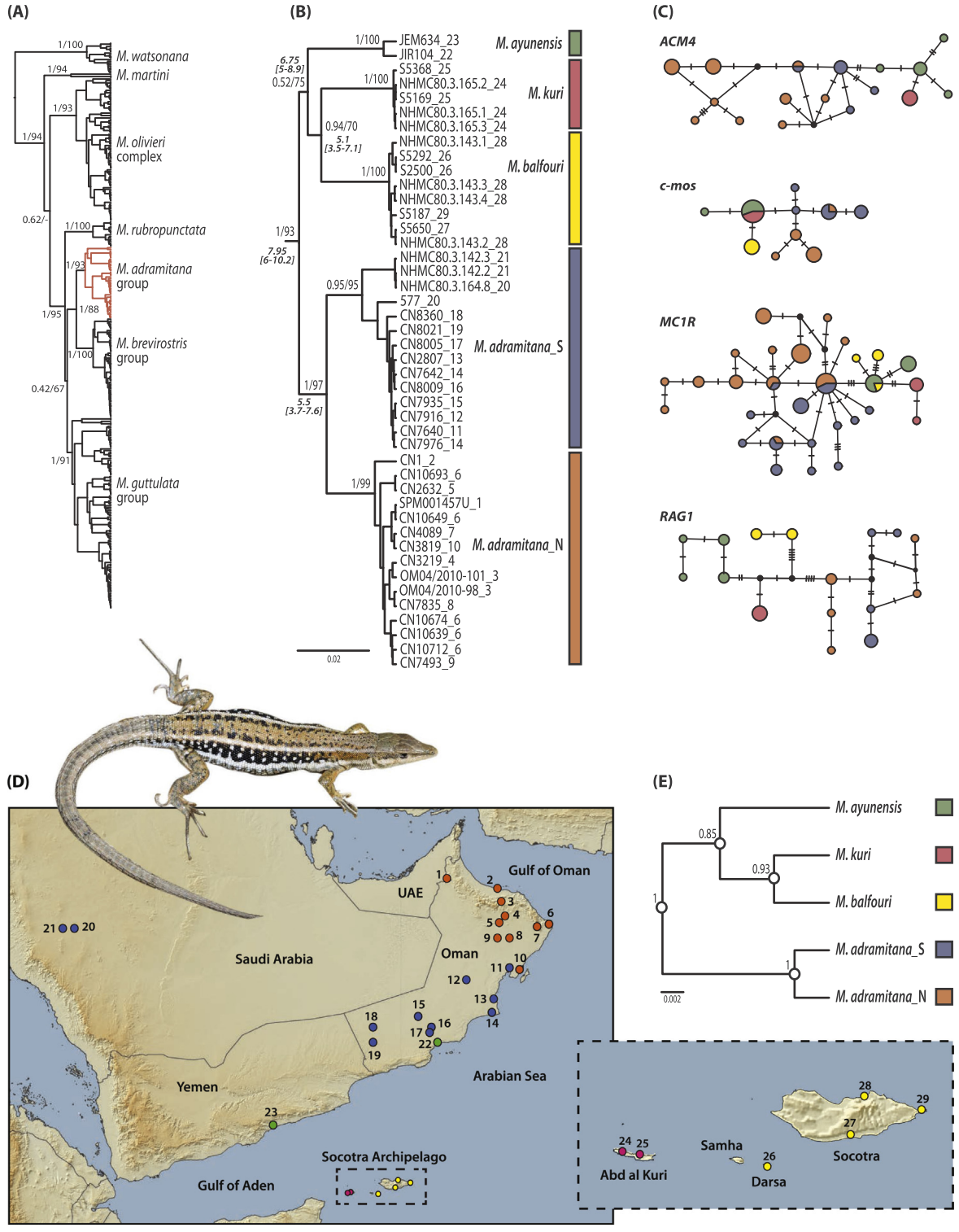

Fig. 2. Results of phylogenetic analyses and geographical distribution of the *Mesalina adramitana* group. (A) Summary Bayesian concatenated tree of *Mesalina* inferred with the complete dataset (dataset 1; see Table S2 for information on the dataset, and Figs. S1 and S2 to see the complete BI and ML trees with information on the tips, respectively). Bootstrap and posterior probability values are indicated near the nodes, respectively. The *M. adramitana* group is highlighted in red. (B) Enlarged Bayesian concatenated tree of the *Mesalina adramitana* group shown in A. Bootstrap and posterior probability values are indicated near the nodes, respectively. Mean age estimates and 95% highest posterior densities inferred with dataset 4 (Table S2 and Fig. 3) are indicated in italics near relevant nodes. Each sample is labelled with the specimen code followed by a locality number (see Table S1 and Fig. 2D). (C) Unrooted haplotype networks of the nuclear markers (*ACM4*, *c-mos*, *MC1R*, *RAG1*) analyzed for the *M. adramitana* group. Circle size is proportional to the number of alleles with colors corresponding to those shown in (B). Small transverse bars show the number of mutational steps between two haplotypes. (D) Localities of the *M. adramitana* group samples with colors corresponding to those shown in (B). (E) *BEAST multilocus species-tree of the *M. adramitana* group inferred with the nuclear genes (dataset 3; Table S2). Posterior probabilities values are indicated above the nodes. White circles indicate nodes with BP&P speciation probabilities of ≥ 0.95 in all analyses. Inset picture shows a specimen of *M. balfouri*. (For interpretation of the references to color in this figure legend, the reader is referred to the web version of this article.)

variable selection (BSSVS; Lemey et al., 2009) implemented in BEAST. In order to account for the different phylogenetic position of *M. martini* in the BI and ML analyses of dataset 1 (see results), the BSSVS analysis was run twice, constraining the topology obtained in the BI and ML trees (only the group comprising *M. martini*). Details on the composition of dataset 4 and on the analyses carried out are specified in Tables S1 and S2. Partitions and models of sequence evolution were inferred in PartitionFinder with the same parameters as detailed above. The calibration points and priors applied to the divergence time analysis have been used in other lacertid studies (e.g., Kaliontzopoulou et al., 2011; Kapli et al., 2015; Tamar et al., 2015, 2016a) and are as follows (for Gallotiinae, Cox et al., 2010; Carranza and Arnold, 2012; for *Podarcis*, Brown et al., 2008): (a) the split between *Gallotia* and *Psammodromus algirus* (age of the oldest of the Canary Islands Fuerteventura and Lanzarote; Normal distribution, mean 18, stdev 2); (b) the split between *G. galloti* and *G. caesaris* (age of La Gomera Island; Normal distribution, mean 6, stdev 3); (c) the split between *G. galloti palmae* and the ancestor of *G. g. galloti* and *G. g. eisentrauti* (age of La Palma Island; Normal distribution, mean 1, stdev 0.5); and (d) the splits between *G. gomerana* and *G. simonyi machadoi* and between *G. caesaris caesaris* and *G. c. gomerae* (age of El Hierro Island; Normal distribution, mean 0.8, stdev 0.2); (e) the separation between *Podarcis pityusensis* and *Podarcis lilfordi* (endemic to the Balearic Islands) at the end of the Messinian Salinity Crisis (Normal distribution, mean 5.32, stdev 0.05). For the ancestral area reconstruction, all *Mesalina* specimens included in dataset 4 were assigned to one of the following four discrete biogeographic areas based on the current distribution of the genus: (1) Asia – Iran to northwest India; (2) Arabia – Iraq to the Sinai Peninsula and the Arabian Peninsula; (3) Socotra Archipelago; and (4) North Africa – Egypt to Mauritania.

2.5. Nuclear networks of the Mesalina adramitana group

Nuclear haplotype networks were constructed to infer the genealogical relationships among the *M. adramitana* group members. To resolve the multiple heterozygous single nucleotide polymorphisms, the on-line web tool SeqPHASE (Flot, 2010) was used to convert the input files, and the software PHASE v.2.1.1 (Stephens et al., 2001; Stephens and Scheet, 2005) to resolve phased haplotypes, with the probability threshold set to 0.7. The phased sequences were used to generate nuclear networks using the TCS statistical parsimony network approach (Clement et al., 2000) in the program Population Analysis with Reticulate Trees (PopART; Leigh and Bryant, 2015).

2.6. Distribution modelling of Mesalina adramitana

Two deeply separated lineages were identified within *M. adramitana* (see results). To assess their distribution and compare environmental niches we first modelled their potential distributions. We used all presence records that were available for *M. adramitana* (Gardner, 2013; Carranza et al., 2018) and that could be assigned to the lineages either based on genetic screening or geographic origin. Both lineages are generally parapatric and some populations in the contact zone that were not sampled for the genetic analyses could not be assigned with certainty to either of them. Therefore, in order not to bias the modelling process by including localities of one lineage in the modelling of the other, we excluded records between 20.258° and 21.746° of latitude (including those from Masirah Island, see Figs. 4 and S4). After removing duplicate entries, the southern lineage had 45 and the northern 113 unique records. To reduce spatial sampling bias with some regions having dense sample coverage (typical for easily accessible urban areas) while others being rather underrepresented, we thinned both data sets separately using the *thin* function of the "spThin" R package (Aiello-Lammens et al., 2015) with a 5 km minimum distance separating any two records. The thinning procedure reduced the number of records to 32 for the southern and 76 for the northern lineage. It is important to note that for the southern lineage we used only the Omani part of its range, firstly because the Saudi populations confirmed to belong to this lineage based on genetic data (Fig. 2; see below) are too geographically disparate from the rest of the species and secondly, the known Yemeni populations have not been screened genetically and their phylogenetic placement thus remains unresolved. The models were developed on a background represented by a 200 km buffer surrounding two convex hulls drawn separately around the southern and northern records (Fig. S4). Variables considered for modelling included the recently derived set of 19 bioclimatic variables (Karger et al., 2017), altitude, slope, and land cover (UN Environment Programme; http://www.unep.org/), all at the finest available resolution of 30 arc sec. We used ENMTools (Warren et al., 2010) to test for spatial correlation between variables and only those with Pearson's $r < 0.75$ and biologically meaningful for the species were retained. Of those, BIO8 (mean temperature of wettest quarter) and BIO18 (precipitation of warmest quarter) presented obvious spatial artifacts with inconsistent spatial patterns, likely due to interpolations, and were not considered in subsequent analyses. The final set used for the modelling contained the following 11 variables: altitude, slope, land cover, BIO3 (isothermality), BIO7 (temperature annual range), BIO10 (mean temperature of warmest quarter), BIO11 (mean temperature of coldest quarter), BIO15 (precipitation seasonality), BIO16 (precipitation of wettest quarter), BIO17 (precipitation of driest quarter), BIO19 (precipitation of coldest quarter). The models were developed using the maximum entropy approach implemented in Maxent v.3.3 (Phillips et al., 2006) with the following settings: maximum number of iterations = 5000; regularization multiplier = 1; maximum number of background points = 10,000; replicates = 10; replicated run type = cross validate. To account for the likelihood of detection of *M. adramitana* in reptile-targeted field surveys conducted in Oman and the UAE in the past two decades we generated a kernel density layer based on all reptile records form these countries (8978 records in total; Fig. S4; Gardner, 2013; Carranza et al., 2018; Burriel-Carranza et al., 2019). We used this layer as a bias file in the modelling process because, as has been shown, including a bias file can substantially improve the quality of model predictions (Kramer-Schadt et al., 2013). The area under the receiver-operating curve (AUC) of each replicate run was taken as a measure of model accuracy and final models were averaged over ten replicates. We reclassified the continuous predictive models into binary presence/absence maps using the maximum training sensitivity plus specificity (MTSS) threshold, which maximizes the combined rate of correctly predicted presences (sensitivity) and absences (specificity) and is considered to accurately predict the potential presence of a species (Jiménez-Valverde and Lobo, 2007). Because the potential niches developed in Maxent may be overpredicted as they do not account for species dispersal limitations or interspecific interactions such as competition (Graham and Hijmans, 2006; Peterson, 2011), we intersected the predicted binary range of each lineage with a 50 km-buffered minimum convex polygon encompassing all records of that lineage. To test whether the predictive models are significantly better than random we generated 100 sets of records randomly distributed in the same study area with the number of records equal to the actual number of records for each lineage (Raes and ter Steege, 2007). We used ENMTools to generate the random sets and run Maxent with the same setting as above. A model is significantly better than random if it ranks among 5% of the best performing models based on random records.

2.7. Identifying dispersal corridors in Mesalina adramitana

To visualize spatial connectivity within the *M. adramitana* lineages while accounting for habitat heterogeneity and its varying role in dispersal in combination with genetic differentiation within each lineage, we calculated least-cost corridors (LCC) among the genetically sampled localities using SDMtoolbox (Brown, 2014) in ArcGIS 10.3 (ESRI, Inc.) (see Chan et al., 2011). We inverted the predictive models of habitat

suitability to create friction layers for the LCC calculations. We used haplotypes of three genes with the best spatial coverage (*12S*, *16S*, *MC1R*) and established corridor layers between two localities that only had shared haplotypes. The percentage of least-cost path value was used to select the LCC with the high, mid, and low cutoff values being respectively 5, 2, and 1. Because the dispersal corridors calculated independently for the *12S*, *16S* and *MC1R* showed congruent spatial patterns, we averaged them to create one population connectivity layer for each *M. adramitana* lineage.

2.8. Niche overlap of Mesalina adramitana

To compare similarity of the niche spaces occupied by the *M. adramitana* lineages we calculated Schoener's D (Schoener, 1968) using ENMTools. This metric permits direct niche comparison by comparing probabilistic distribution models of two species (Warren et al., 2008). Its values range between 0 (no overlap) and 1 (niches identical). To assess whether the predicted distributions exhibit significant ecological differences, we run 100 niche identity tests also in ENMTools. For the identity tests, the two sets of original records are pooled and two new sets are drawn at random, with the number of records in the new sets being identical to the empirical data. Further, to test if the niche similarity or difference is purely a result of environmental conditions available in the geographical regions occupied by the two lineages, we run 100 background tests. The background tests compare a predicted distribution of one species (based on its actual records) with a given number of predicted distributions of the other species, whose records are randomly scattered within its presumed range.

3. Results

3.1. Phylogenetic inference within the genus Mesalina

The overall phylogenetic relationships within *Mesalina* inferred from dataset 1 (the complete *Mesalina* dataset) using the BI and ML methods were mostly concordant across analyses and are presented in Fig. 2A (for full BI and ML trees see Figs. S1 and S2, respectively). We found seven main clades within *Mesalina*: (i) *M. watsonana*, (ii) *M. martini*, (iii) *M. olivieri* complex, (iv) *M. rubropunctata*, and the (v) *M. adramitana*, (vi) *M. brevirostris*, and (vii) *M. guttulata* groups. The seven clades recovered in the BI and ML trees were distinct, well-supported, and mostly consistent with previous studies.

Our phylogenetic analyses (see Figs. S1 and S2) place the Asian *M. watsonana* from Afghanistan, Iran, and Pakistan as sister to the remaining taxa with high support in all analyses. The phylogenetic placement of *M. martini* was less supported and remains unresolved, being either sister to all other taxa except *M. watsonana* in the BI tree, or to the *M. olivieri* complex in the ML tree. The *M. olivieri* complex, distributed mostly across North Africa eastwards to Israel, was well-supported and comprised three non-monophyletic taxa: *M. olivieri*, *M. pasteuri*, and *M. simoni*. The *M. adramitana*, *M. brevirostris*, and *M. guttulata* groups cluster together in one clade in all analyses, being sister to *M. rubropunctata*, although with low support in both BI and ML trees. In all analyses, the *M. guttulata* group was sister to the *M. adramitana* and *M. brevirostris* groups. The Arabian *M. brevirostris* group comprises four species, which are mostly distributed across the Arabian Peninsula and adjoining parts of Iran, with *M. brevirostris* also ranging further east up to central Pakistan. Within this group, *M. bernoullii* was recovered as sister to the remaining taxa and *M. microlepis* was recovered, with low support, as sister to a clade comprising *M. saudiarabica* and *M. brevirostris*. The *M. guttulata* group comprises five species: the Southwest Arabian *M. arnoldi* was recovered as sister to the other taxa, which are divided into two sister clades, the Arabian *M. bahaeldini* with the North African *M. guttulata*, and the South Arabian *M. austroarabica* with the Central and North Arabian *Mesalina* sp. (an unnamed species identified by Sindaco et al., 2018). The relationships within the *M. adramitana* group are described below.

3.2. Phylogeny of the Mesalina adramitana group

Five distinct lineages were found within the *M. adramitana* group, though with a level of allele sharing in the nuclear networks (Fig. 2B and C). The distribution of the five lineages (Fig. 2D) is either in the Arabian Peninsula (i.e., *M. adramitana* from northern Oman, *M. adramitana* from central and southern Oman and western Saudi Arabia, and *M. ayunensis* from southern Oman, and central Yemen), or in the Socotra Archipelago (i.e., *M. balfouri* from Socotra, Samha and Darsa Islands and *M. kuri* from Abd al Kuri Island). Within this group, *M. ayunensis* was recovered as sister to a clade formed by the two Socotran species (*M. balfouri* and *M. kuri*), however, with a low support in the BI analyses. These three taxa cluster together in all the analyses as a sister group to *M. adramitana* (see Fig. 2B). The specimens identified as *M. adramitana* sampled from across Oman were phylogenetically divided into two deep sister lineages (named hereinafter *M. adramitana* North and *M. adramitana* South), a relationship strongly supported in all the analyses performed (Fig. 2B). The contact zone between both lineages is situated south of the Sharqiyah Sands, where two samples from localities 10 and 11 are located, less than 30 km apart at the same latitude (Fig. 2D). The uncorrected genetic distances between these two lineages was relatively high, with 2.9% in *12S*, 4.9% in *16S*, and 11% in *cytb*, and was comparable with the level of genetic variability observed between the other species of the *M. adramitana* group, which ranged

Table 1
Sequence divergence (*p*-distance; in %) derived from the mitochondrial gene fragments of *12S*, *16S*, and *cytb* between and within species that compose the *Mesalina adramitana* group, including the two recognized lineages of *M. adramitana*.

Gene	Taxon	*M. adramitana*_N	*M. adramitana*_S	*M. ayunensis*	*M. balfouri*	*M. kuri*
12S	*M. adramitana*_N	0.37				
	*M. adramitana*_S	2.9	0.28			
	M. ayunensis	2.3	2.5	0.78		
	M. balfouri	4	4.1	4.5	0.48	
	M. kuri	3.1	3.7	4.4	2.7	0
16S	*M. adramitana*_N	0.42				
	*M. adramitana*_S	4.9	1.2			
	M. ayunensis	6.4	5.7	0.23		
	M. balfouri	6.5	6.2	6.8	0.34	
	M. kuri	4.8	4.3	5.7	6.8	0.09
cytb	*M. adramitana*_N	NA				
	*M. adramitana*_S	11	2.54			
	M. ayunensis	10	11	2.99		
	M. balfouri	13.1	12.8	12.4	0.56	
	M. kuri	11.7	10.8	10.9	12.2	0.23

between 2.3 and 4.5% in *12S*, 4.3–6.8% in *16S* and 10–13.1% in *cytb* (see Table 1).

The nuclear networks are presented in Fig. 2C (unfortunately *M. balfouri* could not be amplified for the *ACM4* gene). All haplotypes of *M. ayunensis* in the *ACM4* and *RAG1* nuclear networks were private, but this taxon shares alleles with *M. kuri* and *M. balfouri* in the *c-mos* and the *MC1R* networks, respectively. The sister taxa, *M. kuri* and *M. balfouri*, do not share any alleles in the *c-mos, MC1R* and *RAG1* networks. The results also show that the two deep lineages of *M. adramitana* share alleles in the *ACM4*, *c-mos* and *MC1R* networks, while all haplotypes are private in the *RAG1* network.

The GMYC and bGMYC species delimitation analyses for the entire genus, inferred with dataset 2 (*Mesalina* mitochondrial haplotypes), recovered eight and six mitochondrial lineages within the *M. adramitana* group, respectively (Fig. S3). The more stringent bGMYC results were used in all subsequent analyses, maximizing the reliability of the lineages identified. As explained before, one of these lineages, corresponding to the most isolated populations of *M. adramitana* from Saudi Arabia, was excluded because of the lack of nuclear data (see Table S1). The species-tree inferred with dataset 3 (*M. adramitana* group nuclear dataset) supports the interspecific relationships inferred with the ML and BI methods (Fig. 2B and E). The results of the BP&P species delimitation analyses yielded a model with five putative species and an identical topology to the phylogenetic trees, with consistent results regardless of the analytical approach, the rjMCMC algorithm, the θ and τ priors, and the starting tree used (Fig. 2E).

3.3. Divergence time estimation and biogeographic inference

The GMYC and bGMYC species delimitation analyses for the entire genus (dataset 2) recovered 79 and 52 mitochondrial lineages, respectively (Fig. S3). The divergence time estimation analysis using dataset 4 (complete dataset of bGMYC representatives) indicates that the genus started diversifying during the Oligocene-Miocene transition, approximately 22.7 Mya (17.4–29.2 Mya, 95% highest posterior densities [HPD]; Fig. 3). Deep divergence within the genus appears to have occurred during the Middle-Late Miocene and between the species mostly during the Late Miocene and the Pliocene. The origin of the *M. adramitana* group was estimated to around 8 Mya (95% HPD: 6–10.2 Mya). Colonization of the Socotra Archipelago occurred approximately 7 Mya (95% HPD: 5.4–8.8 Mya), and speciation between *M. kuri* and *M. balfouri* took place ca. 5 Mya (95% HPD: 3.5–7.1 Mya), nearly concurrently with the diversification of the two lineages identified within *M. adramitana* in Arabia (see Fig. 2B).

The BI and ML topologies of the ancestral range reconstructions resulted in almost identical probabilities for the seven main clades within *Mesalina*, though the probabilities of the deeper nodes differed between the two analyses. The biogeographic origin of *Mesalina* was most likely confined to southwestern Asia (with higher probability in the BI topology; Fig. 3). This origin was followed by several radiations within the Arabian Peninsula and North Africa, with numerous dispersal events between both regions. As expected, the *M. adramitana* group most likely originated in the Arabian Peninsula (99%), with a single colonization of the Socotra Archipelago by its continental ancestor.

3.4. Distribution modelling

Maxent produced models of good predictive accuracy for both lineages (i.e., AUC > 0.8; following Araújo et al., 2005) with the AUC means and standard deviations being 0.855 ± 0.041 for the northern and 0.812 ± 0.035 for the southern lineage. The low standard deviation values for both lineages indicate low variance and, therefore, stability of predictions across models. Both models performed significantly better than null models (data not shown). The most important environmental predictors were BIO10 (29.3% contribution), slope (15.1%), and BIO19 (14.9%) for the northern lineage, and BIO19 (47.6%), BIO16 (17.8%), and slope (16.1%) for the southern lineage. The predicted range of *M. adramitana* North covers the flat plains along both sides of the Hajar Mountains (Fig. 4). It stretches in a narrow stripe along the Gulf of Oman from the Musandam Peninsula through Muscat to Ras Al Hadd, the easternmost tip of Oman. West of the Hajar Mountains it extends further to the Persian Gulf coast in the UAE. There is a large isolated patch of suitable habitat in the Ad Dakhiliyah and Ash Sharqiyah North Governorates of Oman west from the Sharqiyah Sands. The habitat identified as suitable for *M. adramitana* South covers most of Dhofar and the southern half of Al Wusta Governorates (Fig. 4 and S4). In most of Dhofar, the potential range is limited to the dry and arid interior of the country and does not extend to the wetter, monsoon-affected, sea side of the mountains. Contrary to the predicted, fragmented, distribution of the northern lineage, the predicted range of the southern lineage is more compact with no disjunct parts (see Fig. 4).

3.5. Dispersal corridors

The dispersal networks for both lineages were correlated with their predictive models, which is not surprising given that the models were used as the input friction layers. The population connectivity layer for the southern lineage shows very little spatial structuring across its predicted range (Fig. 4). On the contrary, that for the northern lineage exhibits a clear pattern of dispersal routes following coastal and lowland areas around and through the Hajar Mountain massifs. The predictive model identified the Hajar Mountains as unsuitable but the dispersal network shows that the wide valleys that cut through the mountain blocks between the Eastern Hajars and Jebel Akhdar (Semail Valley) and at the northern end of the Western Hajars form dispersal corridors that permit gene flow.

3.6. Niche overlap

Niche overlap between the two lineages is relatively low, with Schoener's D = 0.196 (Fig. 5). The niche identity tests yielded D values between 0.663 and 0.882 and the results thus show that the niches of the two lineages are not identical, i.e., are more different than expected by chance. On the contrary, the background tests resulted in very low D values (0.022–0.082 for the original northern records against randomized south; 0.048–0.085 for the original southern records against randomized north), indicating that the niches of the lineages are more similar than expected by the underlying environmental conditions (Fig. 5). Fig. 5 also shows visual comparisons of the niche spaces occupied by the two lineages with respect to the environmental space of the study background.

4. Discussion

Our study constitutes the most up-to-date and comprehensive time-calibrated phylogeny of *Mesalina*. The molecular results are mostly congruent with the current taxonomy and present further undescribed diversity in Arabia, similar to other recent taxonomic studies on this area (Carranza and Arnold, 2012; Šmíd et al., 2017; Metallinou and Carranza, 2013; Vasconcelos and Carranza, 2014; Carranza et al., 2016; Simó-Riudalbas et al., 2017, 2018; Machado et al., 2019; Sindaco et al., 2018). Pending the inclusion of *M. ercolinii*, which is endemic to the Horn of Africa, the genus is currently composed of seven well-supported clades (Fig. 1), including the *M. adramitana* group, one of the main subjects of this work. Discovering hidden diversity highlights the importance of South Arabia as a biodiversity hot spot and a priority focal point for reptile conservation.

4.1. Evolutionary history of the genus Mesalina

Our data support an ancestral diversification of *Mesalina* in

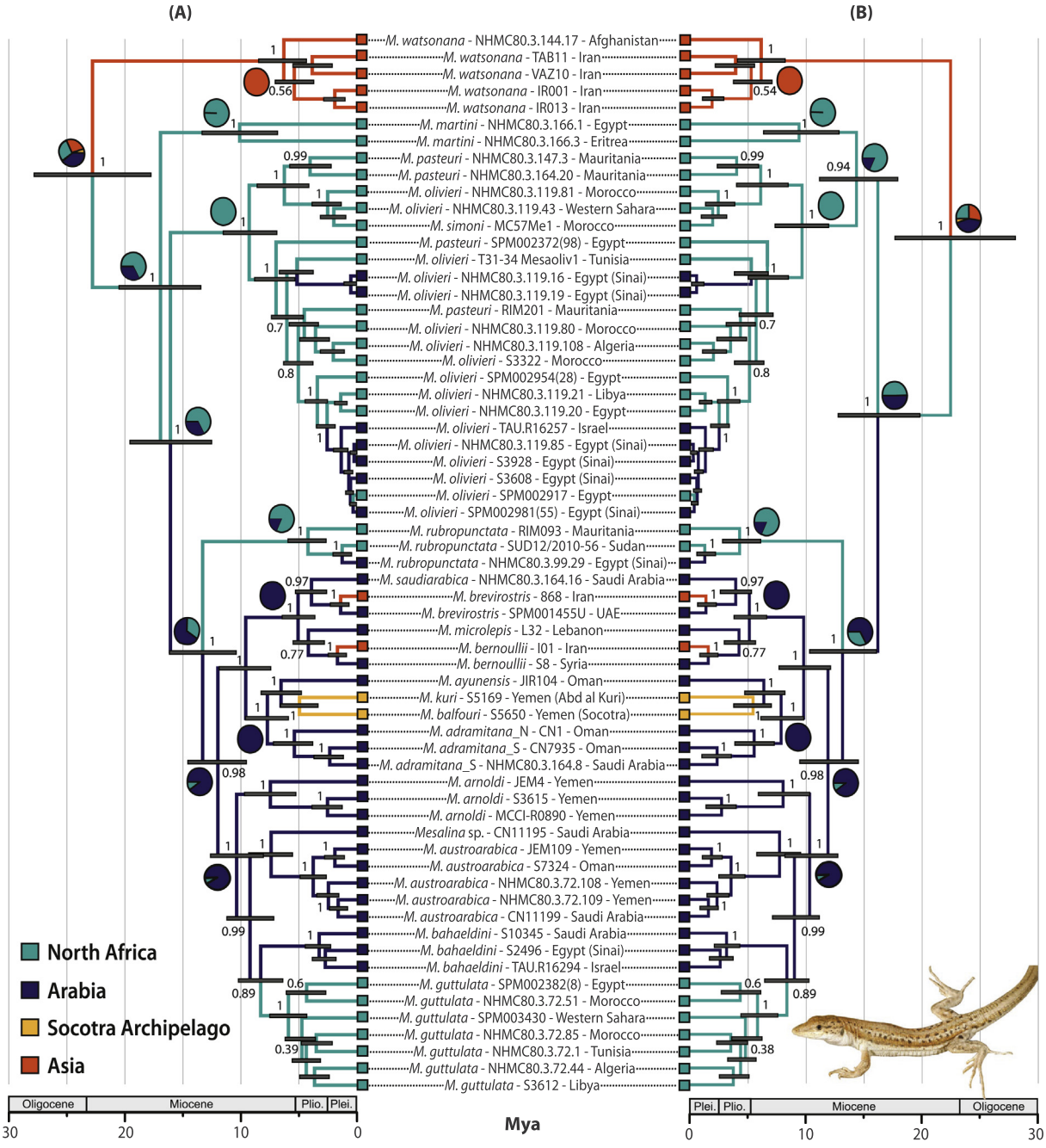

Fig. 3. Ancestral area reconstructions of *Mesalina* inferred with BSSVS using the full dataset of representatives (dataset 4; Table S2). Two topological constraints were enforced according to the BI (A) and ML (B) analyses using dataset 1 (changes in the phylogenetic position of the group comprising *M. martini*). Pie charts describing the probability of ancestral areas are presented near the major nodes (ranges in the lower left legend). Branch colors indicate inferred ancestral range and posterior probability values are indicated above the nodes. Sample codes correspond to those in Table S1. Inset picture shows an individual of *M. kuri*.

southwest Asia during the Oligocene-Miocene transition (23 Mya; similar to Kapli et al., 2015), prior to the formation of the *Gomphotherium* land bridge connecting Afro-Arabia with Eurasia (~15–18 Mya; Rögl, 1999). In this initial split, the ancestor of *M. watsonana*, currently distributed in the Iranian Plateau, diverged from the remaining taxa ranging across Arabia and North Africa (Fig. 3). Following the split of *M. watsonana*, the ancestor of the remaining *Mesalina* taxa diversified during the Miocene and the Pliocene, dispersing back and forth from Arabia to Africa and *vice versa*. This temporal framework is congruent with previous studies on the diversification of North African and Arabian reptiles (e.g., Amer and Kumazawa, 2005; Wüster et al., 2008; Pook et al., 2009; Metallinou et al., 2012, 2015; Portik and Papenfuss 2012, 2015; Šmíd et al., 2013; Tamar et al., 2014, 2016a, 2016b, 2018).

These taxa are divided into three ancestral clades: the *M. olivieri* complex, *M. martini* from North Africa, and a clade including *M. rubropunctata* and the *M. brevirostris*, *M. adramitana*, *M. guttulata* groups from Arabia. The ancestor of the latter clade diverged also during the Middle Miocene (around 13.9 Mya) most likely in Arabia into *M. rubropunctata*, which then dispersed to North Africa, and the Arabian ancestor of the *M. brevirostris*, *M. adramitana*, and *M. guttulata* groups. These groups radiated throughout the Middle-Late Miocene with four dispersals out of Arabia: one of *M. guttulata* to North Africa during the Late Miocene, and another of *M. balfouri* and *M. kuri* to the Socotra Archipelago at the Miocene-Pliocene boundary. Recent dispersals into Asia took place in the *M. brevirostris* group when *M. bernoullii* and *M. brevirostris* colonized Iran in the Pleistocene.

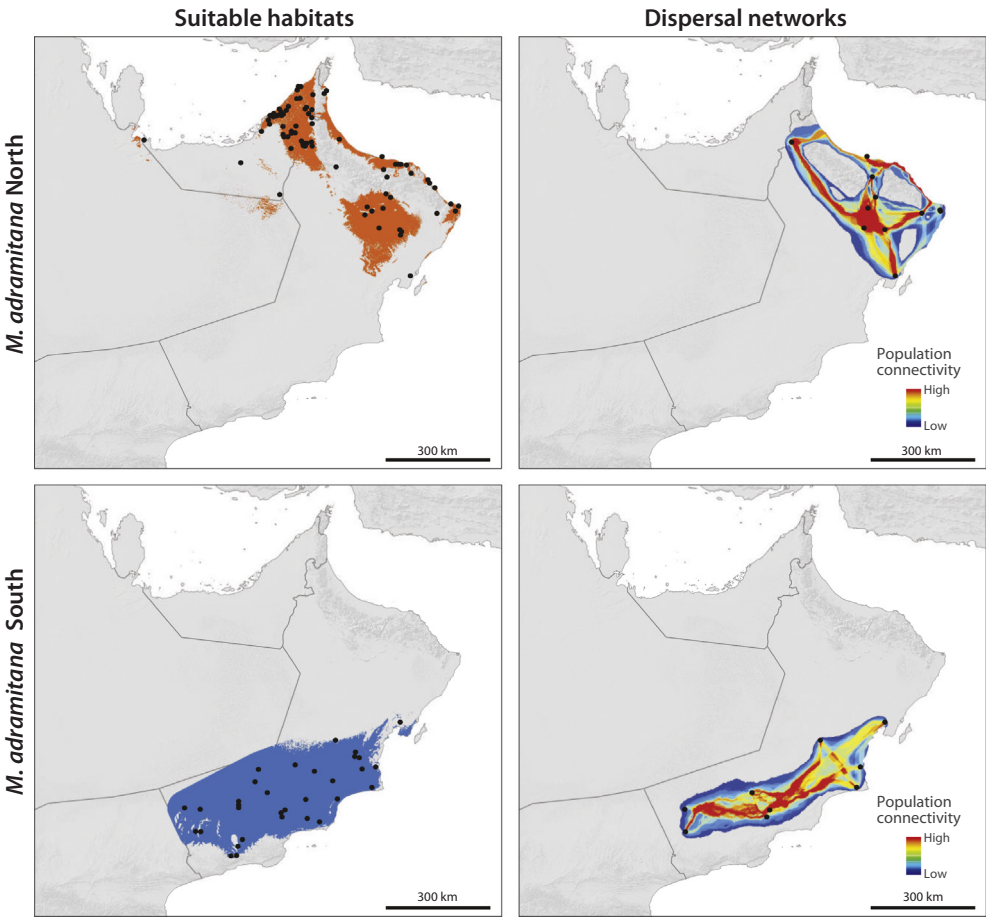

Fig. 4. Distribution models and dispersal corridors of *Mesalina adramitana*. Left panels: Suitable habitats for *M. adramitana* North (upper, orange) and *M. adramitana* South (lower, blue) as identified by distribution modelling and after conversion to binary layers using the MTSS threshold. Black dots indicate localities used for developing the models. Right panels: Dispersal networks for *M. adramitana* North (upper) and South (lower) depicting the connectivity through their suitable habitats. Population connectivity layers were calculated as averages of networks generated independently for the *12S*, *16S* and *MC1R* haplotypes. (For interpretation of the references to color in this figure legend, the reader is referred to the web version of this article.)

As *Mesalina* is an arid-adapted genus preferring hard substrate grounds (Schleich et al., 1996; Baha El Din, 2006; Sindaco and Jeremčenko, 2008), its diversification history was likely influenced by the global climate changes of the Middle-Late Miocene, which led to aridification processes and to the formation and episodic expansions and contractions of the sand deserts in the Arabian Peninsula (Zachos et al., 2001; Griffin, 2002). The complexity of these processes most likely affected the levels of isolation of the *Mesalina* populations, which are delimited by the spatial distribution of the ergs in the Arabian Peninsula (Edgell, 2006). This pattern has also been observed in other widespread reptiles (Amer and Kumazawa, 2005; Carranza et al., 2008; Metallinou et al., 2012, 2015; Tamar et al., 2016a, 2016b, 2018).

4.2. The Mesalina adramitana group

The Arabian *M. adramitana* group comprises four well-defined species: the two endemic species from the Socotra Archipelago (*M. balfouri* and *M. kuri*), the elusive *M. ayunensis* from southern Arabia, and *M. adramitana* with its two deep lineages (*M. adramitana* North and *M. adramitana* South). Similar to previous molecular studies that did not include *M. ayunensis* (Kapli et al., 2008, 2015; Šmíd et al., 2017; Sindaco et al., 2018), *M. kuri* and *M. balfouri* were recovered here as sister taxa. Despite the high levels of diversity and endemicity of the reptiles of the Socotra Archipelago (Razzetti et al., 2011; Vasconcelos et al., 2016), these two species are the only lacertids among the reptiles of this continental archipelago.

The Socotra Archipelago is located in the Arabian Sea, on a continental platform attached to the Horn of Africa, just 100 km from Somalia and 350 km from Arabia. It comprises four islands: Socotra, Samha and Darsa (The Brothers), and Abd al Kuri (Fig. 2D). Once the archipelago became isolated from Arabia (~16–24 Mya), it was subjected to recurrent tectonic events and several marine transgressions that shaped its current geomorphology (Fleitmann et al., 2004). During the last glacial maximum, most of the Socotra platform emerged and a land connection was established between the islands of Socotra, Samha and Darsa creating 'greater Socotra' (Lambeck and Chappell, 2001; Siddall et al., 2004; Cheung and DeVantier, 2006; Van Damme, 2009). On the contrary, Abd al Kuri is isolated from the other islands by deep seas (between 200 and 1000 m deep), exceeding the Pleistocene sea-level changes (Cheung and DeVantier, 2006). Our results support a single colonization of Socotra Archipelago by a long-range transmarine dispersal by an Arabian ancestor approximately 7 Mya, after the archipelago's isolation. *Mesalina kuri* and *M. balfouri* diverged around 5 Mya by a colonization event from Socotra Island to Abd al Kuri or *vice versa*. Despite the recent phylogenetic, phylogeographic, systematic and conservation research on the reptiles of the Socotra Archipelago (Sindaco et al., 2012; Gómez-Díaz et al., 2012; Vasconcelos et al., 2016; Tamar et al., 2019) the genus *Mesalina* is the only example of an intra-archipelago colonization between Socotra and Abd al Kuri Islands.

The mitochondrial and nuclear data clearly suggest an old divergence between the two allopatric lineages found within *M. adramitana* (5.5 Mya; *M. adramitana* North and South), currently distributed from north Oman to the arid regions in the southern part of the country. This divergence is evident in the genetic distance (2.9–10.6% in *12S*, 5.3–14.5% in *16S* and 11.4–21.6% in *cytb*), which is relatively high in comparison to the other recognized species of the *M. adramitana* group (see Table 1). Despite the presence of a narrow contact zone between them (see Fig. 2D), the geographic distributions and environmental niches of *M. adramitana* North and South suggest that environmental conditions have had a strong influence on their differentiation. Both lineages prefer habitats with no slope (e.g., flat plains), as has also been shown for other *Mesalina* species (Hosseinian Yousefkhani et al., 2013).

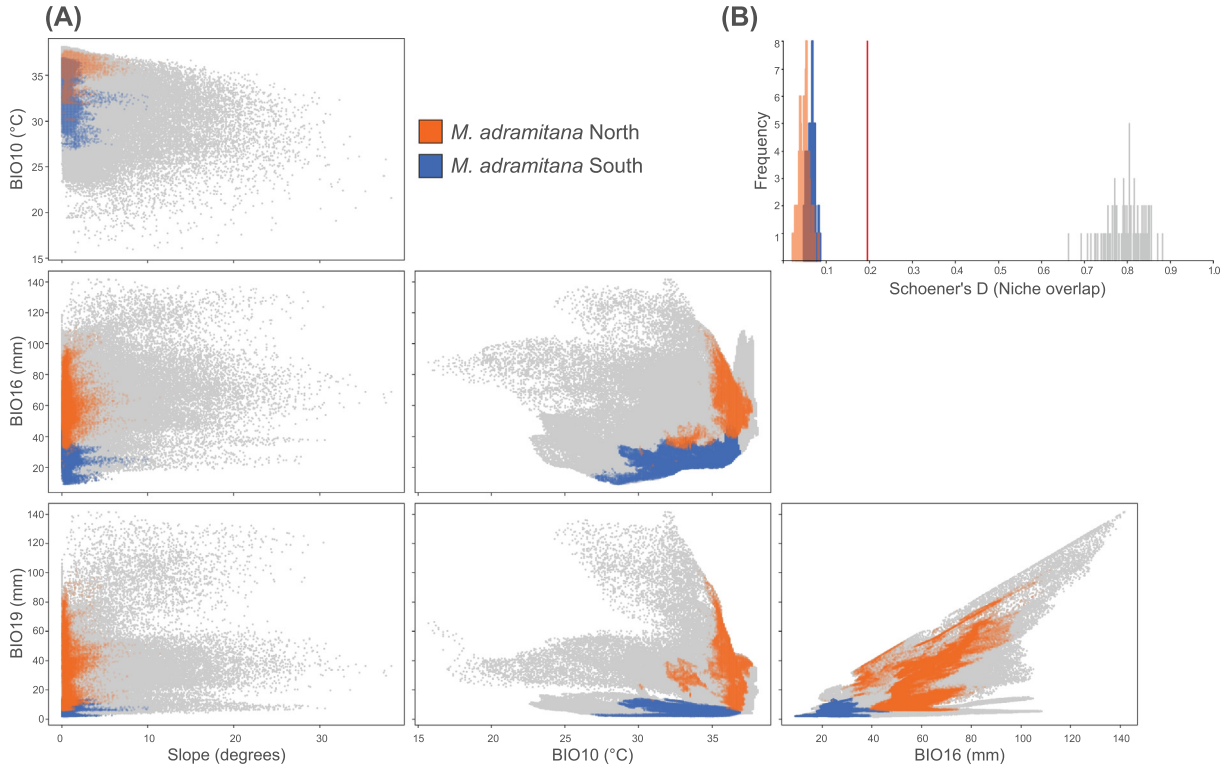

Fig. 5. (A) Scatter plots showing the environmental space of the study background (grey) and its respective parts occupied by the predicted distributions of *M. adramitana* North (orange) and South (blue). The four variables that best predict the potential distributions are plotted. (B) Niche similarity between the two lineages and results of the niche identity and background tests. Red bar shows the actual niche overlap (Schoener's $D = 0.196$). Grey bars are results of the identity tests (100 runs) and show that models based on randomized localities present significantly higher similarity. Orange and blue bars are results of the background tests and show that the niches are more similar than expected by the environmental background in which they occur. Orange bars are for the comparisons of the original *M. adramitana* North records against randomized South (100 runs), blue bars for the original *M. adramitana* South records against randomized North (100 runs). (For interpretation of the references to color in this figure legend, the reader is referred to the web version of this article.)

However, *M. adramitana* South is more tolerant to lower temperatures (BIO10), while *M. adramitana* North generally occurs in areas with over 30 °C in the warmest quarter of the year. Also, *M. adramitana* South can occupy areas with extremely low precipitation, below 20 mm and 40 mm in the coldest (BIO19) and wettest (BIO16) quarter of year, respectively, while *M. adramitana* North prefers higher precipitation (up to 100 mm in both BIO16 and BIO19; Fig. 5A).

The niche comparisons show that the niches of *M. adramitana* North and South are very distinct, yet they are more similar to each other than expected given the environmental conditions of their respective regions. This indicates that the dramatic difference in the niche space of the two lineages is a product of their allopatric distributions, i.e. different parts of the species range have different climate. However, even with such varying climatic conditions across the species range, the niches of *M. adramitana* North and South are more similar than would be expected by chance, which can be taken as evidence for phylogenetic niche conservatism (Warren et al., 2014).

There are no apparent barriers of dispersal within the range of *M. adramitana* South as evidenced by the model of potential distribution and connectivity analysis (Fig. 4). The whole of southern Oman is suitable for this lineage and populations share haplotypes across its entire range, suggesting an isolation-by-distance mode of dispersal. On the contrary, the distribution of the northern lineage surrounds the Hajar Mountains of northern Oman, which are not suitable for the species and therefore form a barrier for dispersal and restrict gene flow. Although altitude does not seem to be the limiting factor, the mountains obviously represent an insurmountable barrier due to their steep slopes. As a result, the northern lineage is more structured with gene flow permitted only along the mountain foothills and through the wadis that cut through between the Eastern Hajars, Jebel Akhdar, and the Western Hajars. A similar pattern has been documented in northern Oman for other groups such as *Trachydactylus* (de Pous et al., 2016), *Asaccus* (Simó-Riudalbas et al., 2018) and *Pristurus* (Garcia-Porta et al., 2017).

Interestingly, in the dry areas of Dhofar, *M. adramitana* South occurs together with *M. ayunensis*, differing from it in several morphological features and habitat occupation (Arnold, 1980). *Mesalina ayunensis* has never been found on the flat areas typical for *M. adramitana* and seems to prefer coarse gravel slopes with scarce vegetation where it is not very abundant (pers. obs.). Despite that a sister relationship between *M. adramitana* and *M. ayunensis* had been suggested (Joger and Mayer, 2002), the considerable geographical variation observed within the former prevented the confirmation of this hypothesis based only on morphological data (Arnold, 1980). Indeed, only *M. adramitana* populations from Dhofar can be easily differentiated from the two other *Mesalina* found in southern Oman (*M. ayunensis* and *M. austroarabica*). Outside this region (i.e., in northern Oman, the UAE and the Hadhramaut area), where the latter two species do not occur, *M. adramitana* overlaps with these species in some morphological traits (Arnold, 1980, 1986a, b). Our molecular results suggest that *M. ayunensis* is a sister taxon to the Socotran species (with apparent nuclear allele sharing between them), forming together a clade sister to *M. adramitana*, even though the support in some of the phylogenetic analyses performed is low. Future studies using additional samples and loci may help estimate the position of *M. ayunensis*. Moreover, for future taxonomic work on the *M. adramitana* group it will be necessary to examine the morphology of the two lineages found within *M. adramitana*, especially from the contact zone in central Oman. Further sampling from the type locality in the Hadhramaut area is required to determine the taxonomic status of the two lineages.

Acknowledgments

We wish to thank Ali Alghafri, Sultan Khalifa, Hamed Al Furkani, Margarita Metallinou, Raquel Vasconcelos, Philip de Pous and Felix Amat for assisting in sample collection in the field. Special thanks are due to Saleh Al Saadi, Salim Bait Bilal, Iman Sulaiman Alazri, Ahmed Said Al Shukaili, Mohammed Al Shariani, Ali Al Kiyumi, Thuraya Al Sariri, Suleiman Nasser Al Akhzami and other members of the Nature Conservation Department of the Ministry of Environment and Climate, Sultanate of Oman for their help and support. Specimens were collected and manipulated with the authorization and under control and permission of the government of Oman (Ministry of Environment and Climate Affairs, MECA). Specimens were captured and processed following the guidelines and protocols stated in the collecting permits and agreements obtained from competent authorities (see references below). All efforts were made to minimize animal suffering. All collecting and export permits were issued by the Nature Conservation Department of the Ministry of Environment and Climate Affairs, Oman (Refs: 08/2005; 16/2008; 38/2010; 12/2011; 13/2013; 21/2013; 37/2014; 31/2016). This work was supported by the Ministerio de Economía y Competitividad, Spain (co-funded by FEDER) under grant numbers CGL2012-36970 and CGL2015-70390-P; Ministry of Environment and Climate Affairs under Grant number 22412027; Secretaria d'Universitats i Recerca del Departament d'Economia i Coneixement de la Generalitat de Catalunya under grant number 2017-SGR-00991. MSR was funded by an FPI grant from the Ministerio de Economía y Competitividad, Spain (BES-2013-064248). JS was funded by the Czech Science Foundation (GACR, project number 18-15286Y) and the Ministry of Culture of the Czech Republic (DKRVO 2019–2023/6.VII.a, 00023272).

Appendix A. Supplementary material

Supplementary data to this article can be found online at https://doi.org/10.1016/j.ympev.2019.04.023.

References

Aiello-Lammens, M.E., Boria, R.A., Radosavljevic, A., Vilela, B., Anderson, R.P., 2015. spThin: an R package for spatial thinning of species occurrence records for use in ecological niche models. Ecography 38, 541–545. https://doi.org/10.1111/ecog.01132.

Amer, S.A.M., Kumazawa, Y., 2005. Mitochondrial DNA sequences of the Afro-Arabian spiny-tailed lizards (genus *Uromastyx*; family Agamidae): phylogenetic analyses and evolution of gene arrangements. Biol. J. Linn. Soc. 85, 247–260. https://doi.org/10.1111/j.1095-8312.2005.00485.x.

Araújo, M.B., Pearson, R.G., Thuiller, W., Erhard, M., 2005. Validation of species–climate impact models under climate change. Glob. Change Biol. 11, 1504–1513. https://doi.org/10.1111/j.1365-2486.2005.01000.x.

Arnold, E.N., 1980. The reptiles and amphibians of Dhofar, southern Arabia. In: Reade S. N., Sale J. B., Gallagher M. D., R. H. Daly (Eds.), The scientific results of the Oman flora and fauna survey 1977 (Dhofar). The Journal of Oman Studies Special Report, 2, 273–332. Muscat, Sultanate of Oman: Office of the Adviser for Conservation of the Environment.

Arnold, E.N., 1986a. A key and annotated checklist to the lizards and amphisbaenians of Arabia. Fauna Saudi Arabia 8, 385–435.

Arnold, E.N., 1986b. Why copulatory organs provide so many useful taxonomic characters: the origin and maintenance of hemipenial differences in lacertid lizards (Reptilia: Lacertidae). Biol. J. Linn. Soc. 29, 263–281. https://doi.org/10.1111/j.1095-8312.1986.tb00279.x.

Arnold, E.N., Arribas, O., Carranza, S., 2007. Systematics of the Palaearctic and Oriental lizard tribe Lacertini (Squamata: Lacertidae: Lacertinae), with descriptions of eight new genera. Zootaxa 1430, 1–86. https://doi.org/10.11646/zootaxa.1430.1.1.

Autin, J., Leroy, S., Beslier, M.O., D'Acremont, E., Razin, P., Ribodetti, A., et al., 2010. Continental break-up history of a deep magma-poor margin based on seismic reflection data (northeastern Gulf of Aden margin, offshore Oman). Geophys. J. Int. 180, 501–519. https://doi.org/10.1111/j.1365-246X.2009.04424.x.

Baha El Din, S., 2006. A Guide to the Reptiles and Amphibians of Egypt. The American University in Cairo Press, Cairo and New York, pp. xvi + 359.

Bohannon, R.G., 1986. Tectonic configuration of the western Arabian continental margin, southern Red Sea. Tectonics 5, 477–499. https://doi.org/10.1029/TC005i004p00477.

Bosworth, W., Huchon, P., McClay, K., 2005. The red sea and Gulf of Aden basins. J. Afr. Earth Sci. 43, 334–378. https://doi.org/10.1016/j.jafrearsci.2005.07.020.

Brown, R.P., Terrasa, B., Pérez-Mellado, V., Castro, J.A., Hoskisson, P.A., Picornell, A., Ramon, M.M., 2008. Bayesian estimation of post-Messinian divergence times in Balearic Island lizards. Mol. Phylogenet. Evol. 48, 350–358. https://doi.org/10.1016/j.ympev.2008.04.013.

Brown, J.L., 2014. SDMtoolbox: a python-based GIS toolkit for landscape genetic, biogeographic and species distribution model analyses. Methods Ecol. Evol. 5, 694–700. https://doi.org/10.1111/2041-210X.12200.

Burriel-Carranza, B., Tarroso, P., Els, J., Gardner, A., Soorae, P., Mohammed, A.A., et al., 2019. An integrative assessment of the diversity, phylogeny, distribution, and conservation of the terrestrial reptiles (Sauropsida, Squamata) of the United Arab Emirates. PloS ONE 14, e0216273. https://doi.org/10.1371/journal.pone.0216273.

Carranza, S., Arnold, E.N., 2012. A review of the gecko genus *Hemidactylus* (Squamata: Gekkonidae) from Oman based on morphology, mitochodrial and nuclear data, with descriptions of eight new species. Zootaxa 95, 1–95.

Carranza, S., Arnold, E.N., Geniez, P., Roca, J., Mateo, J.A., 2008. Radiation, multiple dispersal and parallelism in the skinks, *Chalcides* and *Sphenops* (Squamata: Scincidae), with comments on *Scincus* and *Scincopus* and the age of the Sahara Desert. Mol. Phylogenet. Evol. 46, 1071–1094. https://doi.org/10.1016/j.ympev.2007.11.018.

Carranza, S., Simó-Riudalbas, M., Jayasinghe, S., Wilms, T., Els, J., 2016. Microendemicity in the northern Hajar Mountains of Oman and the United Arab Emirates with the description of two new species of geckos of the genus *Asaccus* (Squamata: Phyllodactylidae). PeerJ 4, e2371. https://doi.org/10.7717/peerj.2371.

Carranza, S., Xipell, M., Tarroso, P., Gardner, A., Arnold, E.N., Robinson, M., et al., 2018. Diversity, distribution and conservation of the terrestrial reptiles of Oman (Sauropsida, Squamata). PLoS ONE 13, e0190389. https://doi.org/10.1371/journal.pone.0190389.

Castresana, J., 2000. Selection of conserved blocks from multiple alignments for their use in phylogenetic analysis. Mol. Biol. Evol. 17, 540–552. https://doi.org/10.1093/oxfordjournals.molbev.a026334.

Chan, L.M., Brown, J.L., Yoder, A.D., 2011. Integrating statistical genetic and geospatial methods brings new power to phylogeography. Mol. Phylogenet. Evol. 59, 523–537. https://doi.org/10.1016/j.ympev.2011.01.020.

Cheung, C., DeVantier, L., 2006. A natural History of hte Islands and their People. Odyssey Books and Guides, Airphoto International Ltd., Hong-Kong.

Clement, M., Posada, D., Crandall, K.A., 2000. TCS: a computer program to estimate gene genealogies. Mol. Ecol. 9, 1657. https://doi.org/10.1046/j.1365-294x.2000.01020.x.

Cox, S.C., Carranza, S., Brown, R.P., 2010. Divergence times and colonization of the Canary Islands by *Gallotia* lizards. Mol. Phylogenet. Evol. 56, 747–757. https://doi.org/10.1016/j.ympev.2010.03.020.

Darriba, D., Taboada, G.L., Doallo, R., Posada, D., 2012. jModelTest 2: more models, new heuristics and parallel computing. Nat. Methods 9, 772. https://doi.org/10.1038/nmeth.2109.

de Pous, P., Machado, L., Metallinou, M., Červenka, J., Kratochvíl, L., Paschou, N., et al., 2016. Taxonomy and biogeography of *Bunopus spatalurus* (Reptilia; Gekkonidae) from the Arabian Peninsula. J. Zool. Syst. Evol. Res. 54, 67–81. https://doi.org/10.1111/jzs.12107.

Douady, C.J., Catzeflis, F., Raman, J., Springer, M.S., Stanhope, M.J., 2003. The Sahara as a vicariant agent, and the role of Miocene climatic events, in the diversification of the mammalian order Macroscelidea (elephant shrews). Proc. Natl. Acad. Sci. 100, 8325–8330. https://doi.org/10.1073/pnas.0832467100.

Drummond, A.J., Suchard, M.A., Xie, D., Rambaut, A., 2012. Bayesian phylogenetics with BEAUti and the BEAST 1.7. Mol. Biol. Evol. 29, 1969–1973. https://doi.org/10.1093/molbev/mss075.

Edgell, H.S., 2006. Arabian Deserts: Nature, Origin and Evolution. Springer, Dordrecht.

Ezard, T., Fujisawa, T. & Barraclough, T.G., 2009. Splits: Species' limits by threshold statistics. R package version, 1. Available from http://R-Forge.R-project.org/projects/splits/.

Fernandes, C.A., Rohling, E.J., Siddall, M., 2006. Absence of post-Miocene Red Sea land bridges: biogeographic implications. J. Biogeogr. 33, 961–966. https://doi.org/10.1111/j.1365-2699.2006.01478.x.

Fleitmann, D., Matter, A., Burns, S.J., Al-Subbary, A., Al-Aowah, M.A., 2004. Geology and Quaternary climate history of Socotra. Fauna Arabia 20, 27–44.

Flot, J.F., 2010. Seqphase: a web tool for interconverting phase input/output files and fasta sequence alignments. Mol. Ecol. Resour. 10, 162–166. https://doi.org/10.1111/j.1755-0998.2009.02732.x.

Fournier, M., Chamot-Rooke, N., Petit, C., Huchon, P., Al-Kathiri, A., Audin, L., et al., 2010. Arabia-Somalia plate kinematics, evolution of the Aden-Owen-Carlsberg triple junction, and opening of the Gulf of Aden. J. Geophys. Res. Solid Earth 115. https://doi.org/10.1029/2008JB006257.

Garcia-Porta, J., Simó-Riudalbas, M., Robinson, M., Carranza, S., 2017. Diversification in arid mountains: biogeography andcryptic diversity of *Pristurus rupestris rupestris* in Arabia. J. Biogeogr. 44, 1694–1704. https://doi.org/10.1111/jbi.12929.

Gardner, A.S., 2013. The Amphibians and Reptiles of Oman and the UAE. Edition Chimaira, Frankfurt am Main, Germany, p. 480.

Gómez-Díaz, E., Sindaco, R., Pupin, F., Fasola, M., Carranza, S., 2012. Origin and in situ diversification in *Hemidactylus* geckos of the Socotra Archipelago. Mol. Ecol. 21, 4074–4092. https://doi.org/10.1111/j.1365-294X.2012.05672.x.

Gonçalves, D.V., Brito, J.C., Crochet, P.A., Geniez, P., Padial, J.M., Harris, D.J., 2012. Phylogeny of North African Agama lizards (Reptilia: Agamidae) and the role of the Sahara desert in vertebrate speciation. Mol. Phylogenet. Evol. 64, 582–591. https://doi.org/10.1016/j.ympev.2012.05.007.

Graham, C.H., Hijmans, R.J., 2006. A comparison of methods for mapping species ranges and species richness. Glob. Ecol. Biogeogr. 15, 578–587. https://doi.org/10.1111/j.1466-8238.2006.00257.x.

Griffin, D.L., 2002. Aridity and humidity: two aspects of the late Miocene climate of North Africa and the Mediterranean. Palaeogeogr. Palaeoclimatol. Palaeoecol. 182, 65–91.

https://doi.org/10.1016/S0031-0182(01)00453-9.
Guillaumet, A., Crochet, P.A., Pons, J.M., 2008. Climate-driven diversification in two widespread Galerida larks. BMC Evol. Biol. 8, 32. https://doi.org/10.1186/1471-2148-8-32.
Guindon, S., Gascuel, O., 2003. A simple, fast, and accurate algorithm to estimate large phylogenies by maximum likelihood. Syst. Biol. 52, 696–704. https://doi.org/10.1080/10635150390235520.
Haq, B.U., Hardenbol, J., Vail, P.R., 1987. Chronology of fluctuating sea levels since the Triassic. Science 235, 1156–1167. https://doi.org/10.1126/science.235.4793.1156.
Harzhauser, M., Kroh, A., Mandic, O., Piller, W.E., Göhlich, U., Reuter, M., Berning, B., 2007. Biogeographic responses to geodynamics: a key study all around the Oligo-Miocene Tethyan Seaway. Zool. Anz. 246, 241–256. https://doi.org/10.1016/j.jcz.2007.05.001.
Harzhauser, M., Piller, W.E., 2007. Benchmark data of a changing sea — palaeogeography, palaeobiogeography and events in the Central Paratethys during the Miocene. Palaeogeogr. Palaeoclimatol. Palaeoecol. 253, 8–31. https://doi.org/10.1016/j.palaeo.2007.03.031.
Heled, J., Drummond, A.J., 2010. Bayesian inference of species trees from multilocusdata. Mol. Biol. Evol. 27, 570–580. https://doi.org/10.1093/molbev/msp274.
Hosseinian Yousefkhani, S.S., Rastegar-Pouyani, E., Rastegar-Pouyani, N., Masroor, R., Šmíd, J., 2013. Modelling the potential distribution of *Mesalina watsonana* (Stoliczka, 1872) (Reptilia: Lacertidae) on the Iranian Plateau. Zoology Middle East 59, 220–228. https://doi.org/10.1080/09397140.2013.841429.
Jiménez-Valverde, A., Lobo, J.M., 2007. Threshold criteria for conversion of probability of species presence to either–or presence–absence. Acta oecologica 31, 361–369. https://doi.org/10.1016/j.actao.2007.02.001.
Joger, U., Mayer, W., 2002. A new species of *Mesalina* (Reptilia: Lacertidae) from Abd al-Kuri, Socotra Archipelago, Yemen, and a preliminary molecular phylogeny for the genus *Mesalina*. Fauna Arabia 19, 497–505.
Jones, R.W., 1999. Marine invertebrate (chiefly foraminiferal) evidence for the palaeogeography of the Oligocene-Miocene of western Eurasia, and consequences for terrestrial vertebrate migration. In: Agustí, J., Rook, L., Andrews, P. (Eds.), Hominoid Evolution and Climatic Change in Europe, The Evolution of Neogene Terrestrial Ecosystems in Europe. Cambridge University Press, London, pp. 274–308.
Kaliontzopoulou, A., Pinho, C., Harris, D.J., Carretero, M.A., 2011. When cryptic diversity blurs the picture: a cautionary tale from Iberian and North African *Podarcis* wall lizards. Biol. J. Linn. Soc. 103, 779–800. https://doi.org/10.1111/j.1095-8312.2011.01703.x.
Kapli, P., Lymberakis, P., Crochet, P.A., Geniez, P., Brito, J.C., Almutairi, M., et al., 2015. Historical biogeography of the lacertid lizard *Mesalina* in North Africa and the Middle East. J. Biogeogr. 42, 267–279. https://doi.org/10.1111/jbi.12420.
Kapli, P., Lymberakis, P., Poulakakis, N., Mantziou, G., Parmakelis, A., Mylonas, M., 2008. Molecular phylogeny of three *Mesalina* (Reptilia: Lacertidae) species (*M. guttulata*, *M. brevirostris* and *M. bahaeldini*) from North Africa and the Middle East: Another case of paraphyly? Mol. Phylogenet. Evol. 49, 102–110. https://doi.org/10.1016/j.ympev.2008.06.016.
Karger, D.N., Conrad, O., Böhner, J., Kawohl, T., Kreft, H., Soria-Auza, R.W., et al., 2017. Climatologies at high resolution for the earth's land surface areas. Sci. Data 4, 170122. https://doi.org/10.1038/sdata.2017.122.
Katoh, K., Standley, D.M., 2013. MAFFT multiple sequence alignment software version 7: improvements in performance and usability. Mol. Biol. Evol. 30, 772–780. https://doi.org/10.1093/molbev/mst010.
Kearse, M., Moir, R., Wilson, A., Stones-Havas, S., Cheung, M., Sturrock, S., et al., 2012. Geneious Basic: an integrated and extendable desktop software platform for the organization and analysis of sequence data. Bioinformatics 28, 1647–1649. https://doi.org/10.1093/bioinformatics/bts199.
van der Kooij, J., 2001. The herpetofauna of the Sultanate of Oman. Part 3: The true lizards, skinks and monitor lizard. Podarcis 2, 15–26.
Kramer-Schadt, S., Niedballa, J., Pilgrim, J.D., Schröder, B., Lindenborn, J., Reinfelder, V., et al., 2013. The importance of correcting for sampling bias in MaxEnt species distribution models. Divers. Distrib. 19, 1366–1379. https://doi.org/10.1111/ddi.12096.
Kumar, S., Stecher, G., Tamura, K., 2016. MEGA7: Molecular Evolutionary Genetics Analysis version 7.0 for bigger datasets. Mol. Biol. Evol. 33, 1870–1874. https://doi.org/10.1093/molbev/msw054.
Lambeck, K., Chappell, J., 2001. Sea level change through the last glacial cycle. Science 292, 679–686. https://doi.org/10.1126/science.1059549.
Lanfear, R., Frandsen, P.B., Wright, A.M., Senfeld, T., Calcott, B., 2016. PartitionFinder 2: new methods for selecting partitioned models of evolution for molecular and morphological phylogenetic analyses. Mol. Biol. Evol. 34, 772–773. https://doi.org/10.1093/molbev/msw260.
Leigh, J.W., Bryant, D., 2015. POPART: full-feature software for haplotype network construction. Methods Ecol. Evol. 6, 1110–1116. https://doi.org/10.1111/2041-210X.12410.
Lemey, P., Rambaut, A., Drummond, A., Suchard, M., 2009. Bayesian phylogeography finds its roots. PLoS Comput. Biol. 5, e1000520. https://doi.org/10.1371/journal.pcbi.1000520.
Machado, L., Šmíd, J., Mazuch, T., Sindaco, R., Al Shukaili, A.S., Carranza, S., 2019. Systematics of the Saharo-Arabian clade of the Palearctic naked-toed geckos with the description of a new species of *Tropiocolotes* endemic to Oman. J. Zool. Syst. Evol. Res. 57, 159–178. https://doi.org/10.1111/jzs.12226.
Mayer, W., Pavlicev, M., 2007. The phylogeny of the family Lacertidae (Reptilia) based on nuclear DNA sequences: convergent adaptations to arid habitats within the subfamily Eremiainae. Mol. Phylogenet. Evol. 44, 1155–1163. https://doi.org/10.1016/j.ympev.2007.05.015.
Metallinou, M., Arnold, E.N., Crochet, P.A., Geniez, P., Brito, J.C., Lymberakis, P., et al., 2012. Conquering the Sahara and Arabian deserts: systematics and biogeography of *Stenodactylus* geckos (Reptilia: Gekkonidae). BMC Evol. Biol. 12, 258. https://doi.org/10.1186/1471-2148-12-258.
Metallinou, M., Carranza, S., 2013. New species of *Stenodactylus* (Squamata: Gekkonidae) from the Sharqiyah Sands in northeastern Oman. Zootaxa 3745, 449–468. https://doi.org/10.11646/zootaxa.3745.4.3.
Metallinou, M., Červenka, J., Crochet, P.A., Kratochvíl, L., Wilms, T., Geniez, P., et al., 2015. Species on the rocks: Systematics and biogeography of the rock-dwelling *Ptyodactylus* geckos (Squamata: Phyllodactylidae) in North Africa and Arabia. Mol. Phylogenet. Evol. 85, 208–220. https://doi.org/10.1016/j.ympev.2015.02.010.
Peterson, A.T., 2011. Ecological niche conservatism: a time-structured review of evidence. J. Biogeogr. 38, 817–827. https://doi.org/10.1111/j.1365-2699.2010.02456.x.
Phillips, S.J., Anderson, R.P., Schapire, R.E., 2006. Maximum entropy modeling of species geographic distributions. Ecol. Model. 190, 231–259. https://doi.org/10.1016/j.ecolmodel.2005.03.026.
Pons, J., Barraclough, T.G., Gomez-Zurita, J., Cardoso, A., Duran, D.P., Hazell, S., et al., 2006. Sequence-based species delimitation for the DNA taxonomy of undescribed insects. Syst. Biol. 55, 595–609. https://doi.org/10.1080/10635150600852011.
Pook, C.E., Joger, U., Stümpel, N., Wüster, W., 2009. When continents collide: phylogeny, historical biogeography and systematics of the medically important viper genus *Echis* (Squamata: Serpentes: Viperidae). Mol. Phylogenet. Evol. 53, 792–807. https://doi.org/10.1016/j.ympev.2009.08.002.
Portik, D.M., Papenfuss, T.J., 2012. Monitors cross the Red Sea: the biogeographic history of *Varanus yemenensis*. Mol. Phylogenet. Evol. 62, 561–565. https://doi.org/10.1016/j.ympev.2011.09.024.
Portik, D.M., Papenfuss, T.J., 2015. Historical biogeography resolves the origins of endemic Arabian toad lineages (Anura: Bufonidae): evidence for ancient vicariance and dispersal events with the Horn of Africa and South Asia. BMC Evol. Biol. 15, 152. https://doi.org/10.1186/s12862-015-0417-y.
Pyron, R.A., Burbrink, F.T., Wiens, J.J., 2013. A phylogeny and revised classification of Squamata, including 4161 species of lizards and snakes. BMC Evol. Biol. 13, 93. https://doi.org/10.1186/1471-2148-13-93.
R Core Team, 2017. R: A language and environment for statistical computing. R Foundation for Statistical Computing, Vienna, Austria. Available from http://www.R-project.org/.
Raes, N., ter Steege, H., 2007. A null-model for significance testing of presence-only species distribution models. Ecography 30, 727–736. https://doi.org/10.1111/j.2007.0906-7590.05041.x.
Rambaut, A., Suchard, M.A., Xie, D. & Drummond, A.J., 2014. Tracer v1.6. Available from http://beast.bio.ed.ac.uk/Tracer.
Razzetti, E., Sindaco, R., Grieco, C., Pella, F., Ziliani, U., Pupin, F., et al., 2011. Annotated checklist and distribution of the Socotran Archipelago Herpetofauna (Reptilia). Zootaxa 2826, 1–44.
Reid, N.M., Carstens, B.C., 2012. Phylogenetic estimation error can decrease the accuracy of species delimitation: a Bayesian implementation of the general mixed Yule-coalescent model. BMC Evol. Biol. 12, 196. https://doi.org/10.1186/1471-2148-12-196.
Rögl, F., 1999. Mediterranean and Paratethys. Facts and hypotheses of an Oligocene to Miocene paleogeography (short overview). Geol. Carpath. 50, 339–349.
Schleich, H., Kastle, W., Kabisch, K., 1996. Amphibians and Reptiles from North Africa. Koeltz Scientific Publishers, Königstein, Germany.
Schoener, T.W., 1968. The *Anolis* lizards of Bimini: resource partitioning in a complex fauna. Ecology 49, 704–726. https://doi.org/10.2307/1935534.
Siddall, M., Smeed, D.A., Hemleben, C., Rohling, E.J., Schmelzer, I., Peltier, W.R., 2004. Understanding the Red Sea response to sea level. Earth Planet. Sci. Lett. 225, 421–434. https://doi.org/10.1016/j.epsl.2004.06.008.
Silvestro, D., Michalak, I., 2012. raxmlGUI: a graphical front-end for RAxML. Org. Divers. Evol. 12, 335–337. https://doi.org/10.1007/s13127-011-0056-0.
Sindaco, R., Jeremčenko, V.K., 2008. The Reptiles of the Western Palearctic: Annotated Checklist and Distributional Atlas of the Turtles, Crocodiles, Amphisbaenians and Lizards of Europe, North Africa, Middle East and Central Asia, vol. 1, Edizioni Belvedere, Latina (Italy), Monografie della Societas Herpetologica Italica, p. 579.
Sindaco, R., Metallinou, M., Pupin, F., Fasola, M., Carranza, S., 2012. Forgotten in the ocean: systematics, biogeography and evolution of the *Trachylepis* skinks of the Socotra Archipelago. Zoolog. Scr. 41, 346–362. https://doi.org/10.1111/j.1463-6409.2012.00540.x.
Sindaco, R., Simó-Riudalbas, M., Sacchi, R., Carranza, S., 2018. Systematics of the *Mesalina guttulata* species complex (Squamata: Lacertidae) from Arabia with the description of two new species. Zootaxa 4429, 513–547. https://doi.org/10.11646/zootaxa.4429.3.4.
Simó-Riudalbas, M., Metallinou, M., de Pous, P., Els, J., Jayasinghe, S., Péntek-Zakar, E., Wilms, T., Al-Saadi, S., Carranza, S., 2017. Cryptic diversity in *Ptyodactylus* (Reptilia: Gekkonidae) from the northern Hajar Mountains of Oman and the United Arab Emirates uncovered by an integrative taxonomic approach. PLoS ONE 12, e0180397. https://doi.org/10.1371/journal.pone.0180397.
Simó-Riudalbas, M., Tarroso, P., Papenfuss, T., Al-Sariri, T., Carranza, S., 2018. Systematics, biogeography and evolution of *Asaccus gallagheri* (Squamata, Phyllodactylidae) with the description of a new endemic species from Oman. Syst. Biodivers. 16, 323–339. https://doi.org/10.1080/14772000.2017.1403496.
Šmíd, J., Carranza, S., Kratochvíl, L., Gvoždík, V., Nasher, A.K., Moravec, J., 2013. Out of Arabia: A Complex Biogeographic History of Multiple Vicariance and Dispersal Events in the Gecko Genus *Hemidactylus* (Reptilia: Gekkonidae). PLoS ONE 8, e64018. https://doi.org/10.1371/journal.pone.0064018.
Šmíd, J., Frynta, D., 2012. Genetic variability of *Mesalina watsonana* (Reptilia: Lacertidae) on the Iranian plateau and its phylogenetic and biogeographic affinities as inferred from mtDNA sequences. Acta Herpetologica 7, 139–153. https://doi.org/10.13128/

Acta_Herpetol-10193.
Šmíd, J., Moravec, J., Gvoždík, V., Štundl, J., Frynta, D., Lymberakis, P., et al., 2017. Cutting the Gordian Knot: Phylogenetic and ecological diversification of the *Mesalina brevirostris* species complex (Squamata, Lacertidae). Zoolog. Scr. 46, 649–664. https://doi.org/10.1111/zsc.12254.
Stamatakis, A., 2014. RAxML version 8: a tool for phylogenetic analysis and post-analysis of large phylogenies. Bioinformatics 30, 1312–1313. https://doi.org/10.1093/bioinformatics/btu033.
Stephens, M., Scheet, P., 2005. Accounting for decay of linkage disequilibrium in haplotype inference and missing-data imputation. Am. J. Human Genet. 76, 449–462. https://doi.org/10.1086/428594.
Stephens, M., Smith, N.J., Donnelly, P., 2001. A new statistical method for haplotype reconstruction from population data. Am. J. Human Genet. 68, 978–989. https://doi.org/10.1086/319501.
Talavera, G., Castresana, J., 2007. Improvement of phylogenies after removing divergent and ambiguously aligned blocks from protein sequence alignments. Syst. Biol. 56, 564–577. https://doi.org/10.1080/10635150701472164.
Tamar, K., Carranza, S., Sindaco, R., Moravec, J., Meiri, S., 2014. Systematics and phylogeography of *Acanthodactylus schreiberi* and its relationships with *Acanthodactylus boskianus* (Reptilia: Squamata: Lacertidae). Zool. J. Linn. Soc. 172 (3), 720–739. https://doi.org/10.1111/zoj.12170.
Tamar, K., Carranza, S., Sindaco, R., Moravec, J., Meiri, S., 2015. Hidden relationships and genetic diversity: Molecular phylogeny and phylogeography of the Levantine lizards of the genus *Phoenicolacerta* (Squamata: Lacertidae). Mol. Phylogenet. Evol. 91, 86–97. https://doi.org/10.1016/j.ympev.2015.05.002.
Tamar, K., Carranza, S., Sindaco, R., Moravec, J., Trape, J.F., Meiri, S., 2016a. Out of Africa: phylogeny and biogeography of the widespread genus *Acanthodactylus* (Reptilia: Lacertidae). Mol. Phylogenet. Evol. 103, 6–18. https://doi.org/10.1016/j.ympev.2016.07.003.
Tamar, K., Metallinou, M., Wilms, T., Schmitz, A., Crochet, P.A., Geniez, P., Carranza, S., 2018. Evolutionary history of spiny-tailed lizards (Agamidae: *Uromastyx*) from the Saharo-Arabian region. Zoolog. Scr. 47, 159–173. https://doi.org/10.1111/zsc.12266.
Tamar, K., Scholz, S., Crochet, P.A., Geniez, P., Meiri, S., Schmitz, A., Wilms, A., Carranza, S., 2016b. Evolution around the Red Sea: Systematics and biogeography of the agamid genus *Pseudotrapelus* (Squamata: Agamidae) from North Africa and Arabia. Mol. Phylogenet. Evol. 97, 55–68. https://doi.org/10.1016/j.ympev.2015.12.021.
Tamar, K., Simó-Riudalbas, M., Garcia-Porta, J., Santos, X., Llorente, G., Vasconcelos, R., et al., 2019. An integrative study of island diversification: insights from the endemic *Haemodracon* geckos of the Socotra Archipelago. Mol. Phylogenet. Evol. 133, 166–175. https://doi.org/10.1016/j.ympev.2019.01.009.
Tonini, J.F.R., Beard, K.H., Ferreira, R.B., Jetz, W., Pyron, R.A., 2016. Fully-sampled phylogenies of squamates reveal evolutionary patterns in threat status. Biol. Conserv. 204, 23–31. https://doi.org/10.1016/j.biocon.2016.03.039.
Uetz, P., Freed, P., Hzrošek, J., 2017. The Reptile database. Retrieved from http://www.reptile-database.org.
Van Damme, K., 2009. Socotra archipelago. In: Gillespie, R.G., Clague, D.A. (Eds.), Encyclopedia of Islands. University of California Press, Berkeley &, Los Angeles, California, pp. 846–851.
Vasconcelos, R., Carranza, S., 2014. Systematics and biogeography of *Hemidactylus homoeolepis* Blanford, 1881 (Squamata: Gekkonidae), with the description of a new species from Arabia. Zootaxa 3835, 501–527. https://doi.org/10.11646/zootaxa.3835.4.4.
Vasconcelos, R., Montero-Mendieta, S., Simó-Riudalbas, M., Sindaco, R., Santos, X., Fasola, M., et al., 2016. Unexpectedly high levels of cryptic diversity uncovered by a complete DNA barcoding of reptiles of the Socotra Archipelago. PLoS ONE 11, e0149985. https://doi.org/10.1371/journal.pone.0149985.
Warren, D.L., Cardillo, M., Rosauer, D.F., Bolnick, D.I., 2014. Mistaking geography for biology: inferring processes from species distributions. Trends Ecol. Evol. 29, 572–580. https://doi.org/10.1016/j.tree.2014.08.003.
Warren, D.L., Glor, R.E., Turelli, M., 2008. Environmental niche equivalency versus conservatism: quantitative approaches to niche evolution. Evolution 62, 2868–2883. https://doi.org/10.1111/j.1558-5646.2008.00482.x.
Warren, D.L., Glor, R.E., Turelli, M., 2010. ENMTools: a toolbox for comparative studies of environmental niche models. Ecography 33, 607–611. https://doi.org/10.1111/j.1600-0587.2009.06142.x.
Wüster, W., Peppin, L., Pook, C.E., Walker, D.E., 2008. A nesting of vipers: phylogeny and historical biogeography of the Viperidae (Squamata: Serpentes). Mol. Phylogenet. Evol. 49, 445–459. https://doi.org/10.1016/j.ympev.2008.08.019.
Yang, Z., Rannala, B., 2010. Bayesian species delimitation using multilocus sequence data. Proc. Natl. Acad. Sci. 107, 9264–9269. https://doi.org/10.1073/pnas.0913022107.
Yang, Z., Rannala, B., 2014. Unguided species delimitation using DNA sequence data from multiple loci. Mol. Biol. Evol. 31, 3125–3135. https://doi.org/10.1093/molbev/msu279.
Zachos, J., Pagani, M., Sloan, L., Thomas, E., Billups, K., 2001. Trends, rhythms, and aberrations in global climate 65 Ma to present. Science 292, 686–693. https://doi.org/10.1126/science.1059412.